Influence of structure-foundation-soil interaction on ground motions recorded within buildings

Dimitris Sotiriadis[1], Nikolaos Klimis[1], Basil Margaris[2] and Anastasios Sextos[3,4]

[1] Department of Civil Engineering, Democritus University of Thrace, Greece.

[2] Institute of Engineering Seismology and Earthquake Engineering (ITSAK-EPPO), Thessaloniki, Greece.

[3] Department of Civil Engineering, University of Bristol, UK.

[4] Department of Civil Engineering, Aristotle University of Thessaloniki, Greece.

Abstract

The present work investigates the effect of soil – structure interaction (SSI) on foundation motion recorded at accelerometric stations installed at the lowest level of buildings. For this purpose, two sites of instrumented buildings, for which foundation and free-field strong motion recordings are available, are studied in terms of transfer functions as well as strong motion intensity and frequency content. The importance of such an instrumentation scheme is highlighted, especially when it comes to assessing the filtering action of the foundation on moderate to high frequency components of free-field motions. The effect of ground motion filtering at the soil-foundation interface is further quantified in terms of amplitude and frequency content. The recordings are supplemented by a parametric analysis of the sub-structured soil-structure system leading to regression expressions that associate the intensity and frequency parameters of the recordings obtained at the base of the instrumented buildings and the corresponding free-field ones. It is shown that kinematic and inertial decoupling of SSI is not only a useful but also a necessary task for correcting earthquake records obtained at building basements particularly for high frequency-dominated ground motions.

Keywords

Soil-structure interaction; strong motion recordings; embedded foundations; numerical sub-structuring

1. INTRODUCTION

Soil-structure interaction (SSI) refers to the coupled dynamic effect between a superstructure, its foundation and supporting soil that tend to act as a system thus affecting the seismic response of all individual components. As shown in Veletsos et al. (1974), Bielak (1974), Mylonakis et al. (2006) and Kim and Stewart (2003) the modification of the dynamic response of a structure supported on compliant soil with respect to the fixed base approach consists of: (i) the fundamental period elongation of the system, (ii) the apparent increase in damping due to wave radiation and inelastic soil response and (iii) the filtering of the incident waves arriving at the base of the structure, as a result of both base-slab averaging and embedment effects.

This problem has been extensively studied though both holistic and sub-structuring techniques. According to the latter, the foundation motion is treated as the combination of two phenomena that in essence occur simultaneously but are analytically decoupled in two subsequent phases: *kinematic interaction*, where the soil motion is modified, effectively filtered, due to the presence of a massless, rigid foundation, resulting into the Foundation Input Motion (FIM) which is used as the earthquake input for the flexibly supported superstructure forming the *inertial interaction* phase. Naturally, FIM is also modified due to seismic waves radiated back to the soil due to the oscillation of superstructure and is calculated in cases where the foundation response is of interest.

Foundation Input Motion is different to that of the nearby free-field ground motion in terms of frequency, amplitude and phase. The frequency-dependent response amplitude of the FIM over that of the free-field is often expressed by means of a transfer function in the frequency domain that has been found approximately equal to unity for low frequencies, while tending to reduce with increasing frequency, at least for uniform soils. The FIM, apart from translational motions, includes also rotational (rocking, torsional) components which are amplified for higher frequencies and should be considered when kinematic interaction is accounted for (Kim and Stewart, 2003; Mylonakis et al., 2006). Many analytical studies reported in the literature have addressed the case of rigid foundations of various shapes, embedded or lying on the surface of a uniform or layered half-space, excited by vertically propagating or inclined wave fields (Trifunac, 1972; Elsabee et al., 1977; Luco and Wong, 1987; Veletsos et al, 1997; Hossein and Pouran, 2017; Conti et al., 2017, Conti et al., 2018).

An integral part of the substructure analysis process, is the replacement of the surrounding soil by frequency-dependent impedance functions that typically define the properties of coupled springs and dashpots at the base of the structure-foundation interface. Many analytical expressions and procedures have been developed over the years investigating various parameters that control their properties in the frequency domain (Luco, 1974; Kausel, 1978; Wolf and Somaini, 1986; Dobry and Gazetas, 1986; Pais and Kausel, 1988; Gazetas, 1991; Mylonakis et al., 2006) while more recent efforts have led to the use of frequency-dependent Lumped Parameter Models that can be also used in the time domain (Lesgidis et al., 2015; 2016; 2018). Having determined the properties of the FIM and the impedance functions, the coupled response of the foundation is computed through dynamic analysis of a system which includes the flexibly supported superstructure and excited by the FIM.

Apart from analytical studies, strong motion recordings at both foundation level and free-field, have been utilized to assess the degree of coupling between the superstructure, foundation and free-field motion through a transfer function or response/floor spectra (Luco et al., 1990; Talaganov and Cubrinovski, 1991; Stewart et al., 1998). Other recordings have been used to calibrate existing analytical models (Kim and Stewart, 2003). Albeit important focus has been made to the proper estimation of the transfer function between the foundation and the free-field motion in the frequency domain, research is currently limited on assessing the correlation between the foundation and free-field motion intensity and frequency content parameters (Sarma and Srbulov, 1996; Stewart et al., 1998; Yamada et al., 2016).

Along these lines, the objective of this paper is to correlate ground motion properties using, as a case study test-bed, the recordings of the Hellenic National Accelerometric Network (HNAN) in Greece, run by the Institute of Engineering Seismology and Earthquake Engineering (ITSAK-EPPO) obtained at the basement of carefully instrumented and documented single or multi-storey buildings. A wider aim, that is not exhausted in this work but highlights its importance, is the possibility to use the outcomes of the SSI impact on the earthquake records obtained within instrumented buildings to draw corrective procedures that can predict the equivalent "building-free" ground motions and assess the error induced by SSI on Ground Motion Prediction Equations (GMPEs) and seismic hazard that have been produced utilizing uncorrected suites of ground motions (Boore et al., 2014).

Towards the above objectives, two sites in Greece are studied, for which foundation and free-field strong motion recordings are available. Initially, the strong motion recordings are utilized to obtain the recorded transfer functions in order to highlight the modification of the foundation motion with respect to the free-field, as a consequence of SSI. Subsequently, a sub-structure analysis is employed to estimate the corresponding transfer function for each site. The analytical transfer functions are then compared to those obtained from the recordings and the predictive capability of the analytical approach is assessed. Finally, parametric analyses of the sub-structured system are conducted for each site to derive correlating expressions that relate intensity and frequency content parameters of the foundation and the free-field motions compare them with the available strong motion data.

2. ACCELEROMETRIC STATIONS STUDIED

Two specific sites are considered in this study both including at least one accelerographic station located at the base of the building and one free field station. The sites studied are referred as Cosmos Offices (CO) in Thessaloniki and Lefkada's administration building (LAB) and are described in the following.

2.1 Cosmos Offices

2.1.1 Building description

The CO building is located at the municipality of Pilea, on the east side of the city of Thessaloniki in Greece. It is a reinforced concrete building consisting of three storeys and a basement. The plan dimensions of the building, along with the accelerographic stations' position are given in Fig. 1.

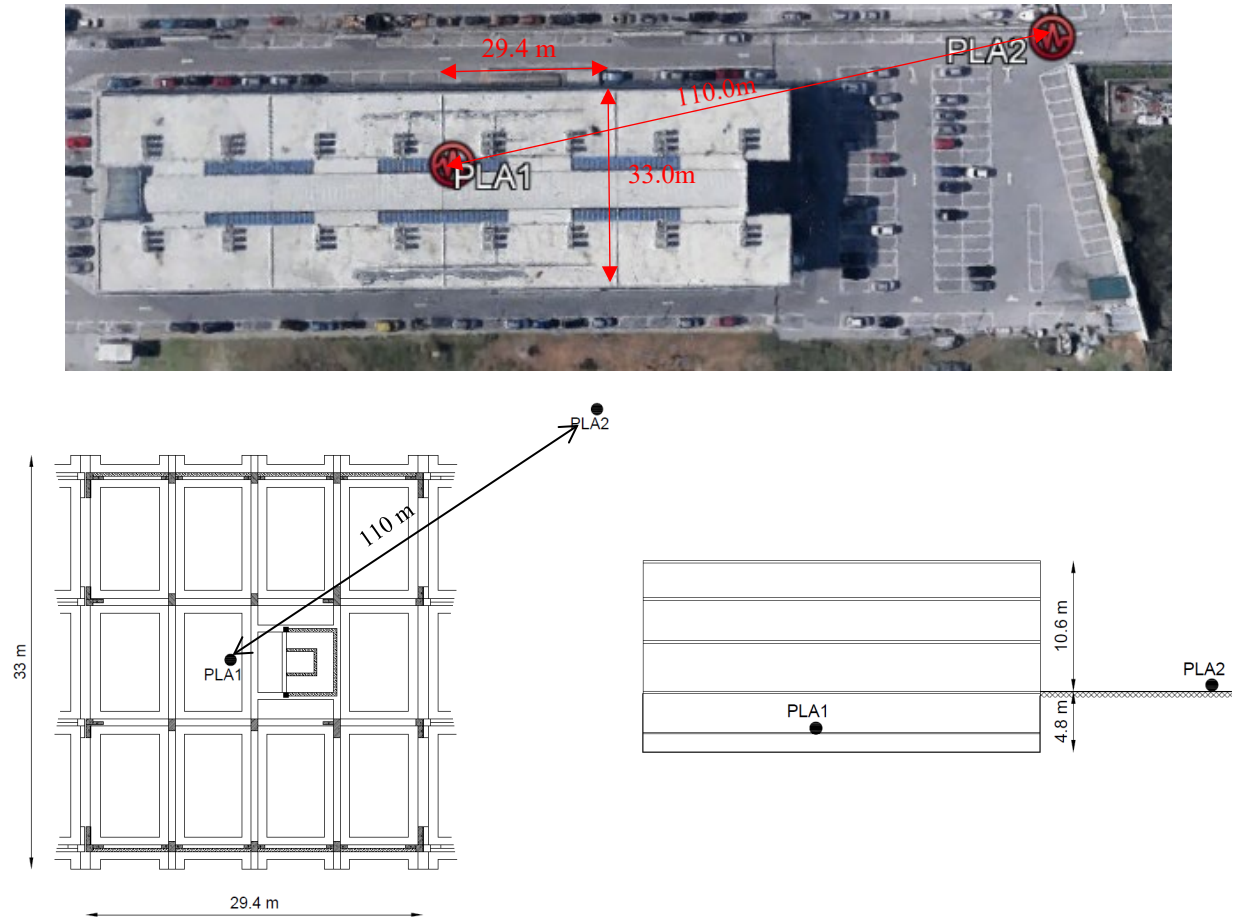

Fig. 1 Plan dimensions and accelerographic stations' (PLA1 and PLA2) position at the site of Cosmos Offices. Top: top view of site along with building dimensions and relative distance between stations PLA1 and PLA2. Bottom left: plan view of building foundation and corresponding dimensions. Bottom right: schematic elevation of Cosmos offices bulding.

The building complex consists of similar, statically independent buildings with plan dimensions 29.4m x 33.0m (transverse x longitudinal). Along the transverse direction, the buildings are positioned one next to the other with a 10cm wide constructional joint separating them that ensures their static independence. The total height of the building is equal to 10.99 m. The foundation of the building consists of a grid of strip foundations on which vertical structural elements are supported. The width of the strip foundation varies from 2.0 to 2.60m whereas their cross-section height is equal to 1.50m. The stairway and the elevator core are supported by a rectangular footing which is connected to the foundation grid through link beams. The foundation depth is at -4.8m. The computational model of the building was formed based on the structural design report and the construction drawings. The estimated mass of each floor is shown in Table 1.

Table 1 Floor mass of Cosmos Offices building

STOREY	MASS (tons)
1	823.56
2	807.30
3	700.34
Foundation	2198.42

The uncoupled fundamental periods along the two principal directions of the building were calculated through modal analysis, as $T_{1,long}$=0.46sec and $T_{1,transv}$=0.30sec.

2.1.2 Soil profile

The shear wave velocity (V_s) profile was available only for the first 30m below the ground surface (Conti et al., 2018; Fig. 2) while the average value of V_s at the upper 30m equal to $V_{s,30}$=266m/sec.

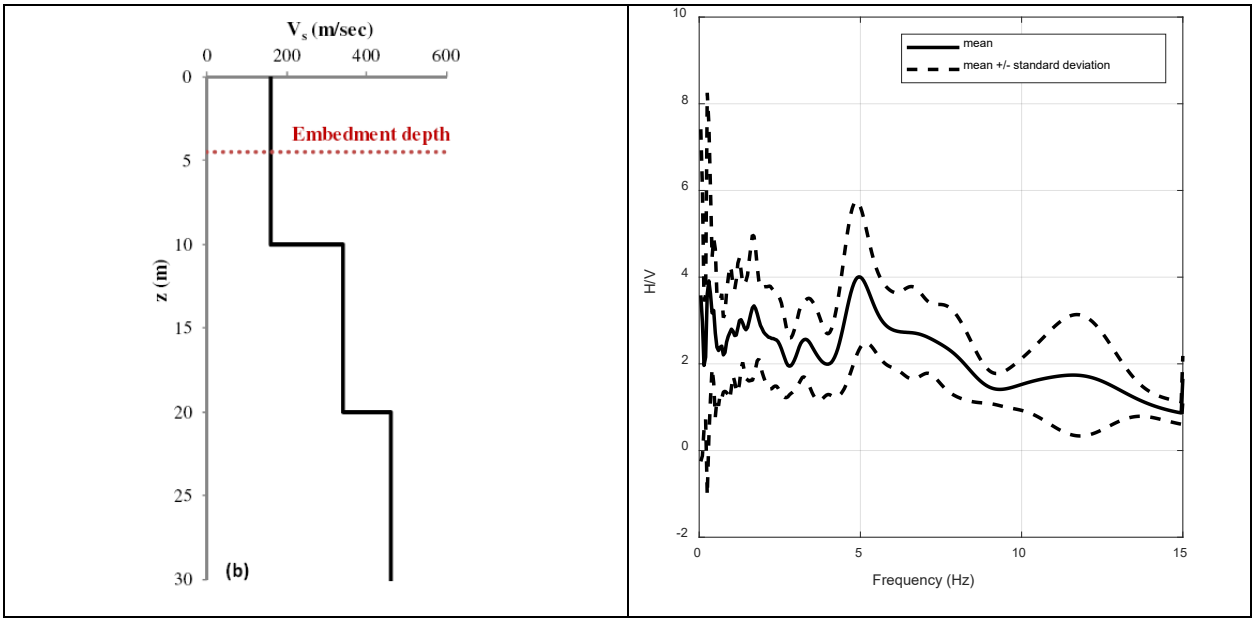

Fig. 2 **Left:** shear wave velocity profile at the Cosmos Offices site (Conti et al., 2018). Right: H/V ratio computed through the recordings of the free-field station (PLA2)

According to the soil type classification of Eurocode 8 (EN1998-1), the CO profile is classified as type C which refers to deep deposits of dense or medium dense sand, gravel or stiff clay with thickness from several tens to many hundreds of meters. Soil sections of a nearby area, proposed by Manakou et al. (2008), confirm that soil deposits may reach several hundreds of meters. This is also indicated by the H/V ratios (Nakamura, 1989) calculated through the recordings of the free-field station. Further information on soil engineering properties was extracted from the Engineering Geological Map of the Institute of Geology and Mineral Exploration. (IGME, 1993).

2.2 Lefkada's Administration Building

2.2.1 Building Description

The administration building at the island of Lefkada is made of reinforced concrete and consists of 2 storeys and one basement. The plan dimension of the building, along with the accelerographic stations' position, is depicted in Fig. 3. The typical floor plan of the building is irregular in shape with approximate dimensions 24.65x46.8m (transverse x longitudinal). The structural system consists of structural walls in both principal directions. The total height of the structure is equal to 8.3m. The foundation is composed of a grid of strip footings with width varying from 1.15-2.10m, a height of 1.5m and is embedded at a depth of 5m.

The dynamic characteristics of the building were computed based on the constructional drawings which were made available by the local authorities. The mass of each floor was calculated and is reported in Table 2. The uncoupled fundamental periods along the two principal directions of the building were calculated through modal analysis, as $T_{1,trans}$=0.138s and $T_{1,long}$=0.137s. These results agree well with the work of Karakostas et al. (2017) who have performed SSI analyses on this site with a breadth of modeling approaches.

Table 2 Floor mass of administration building in the island of Lefkada (LAB).

STOREY	m (tons)
Foundation	1306.61
Ground floor	974.09
1	881.49
2	670.99

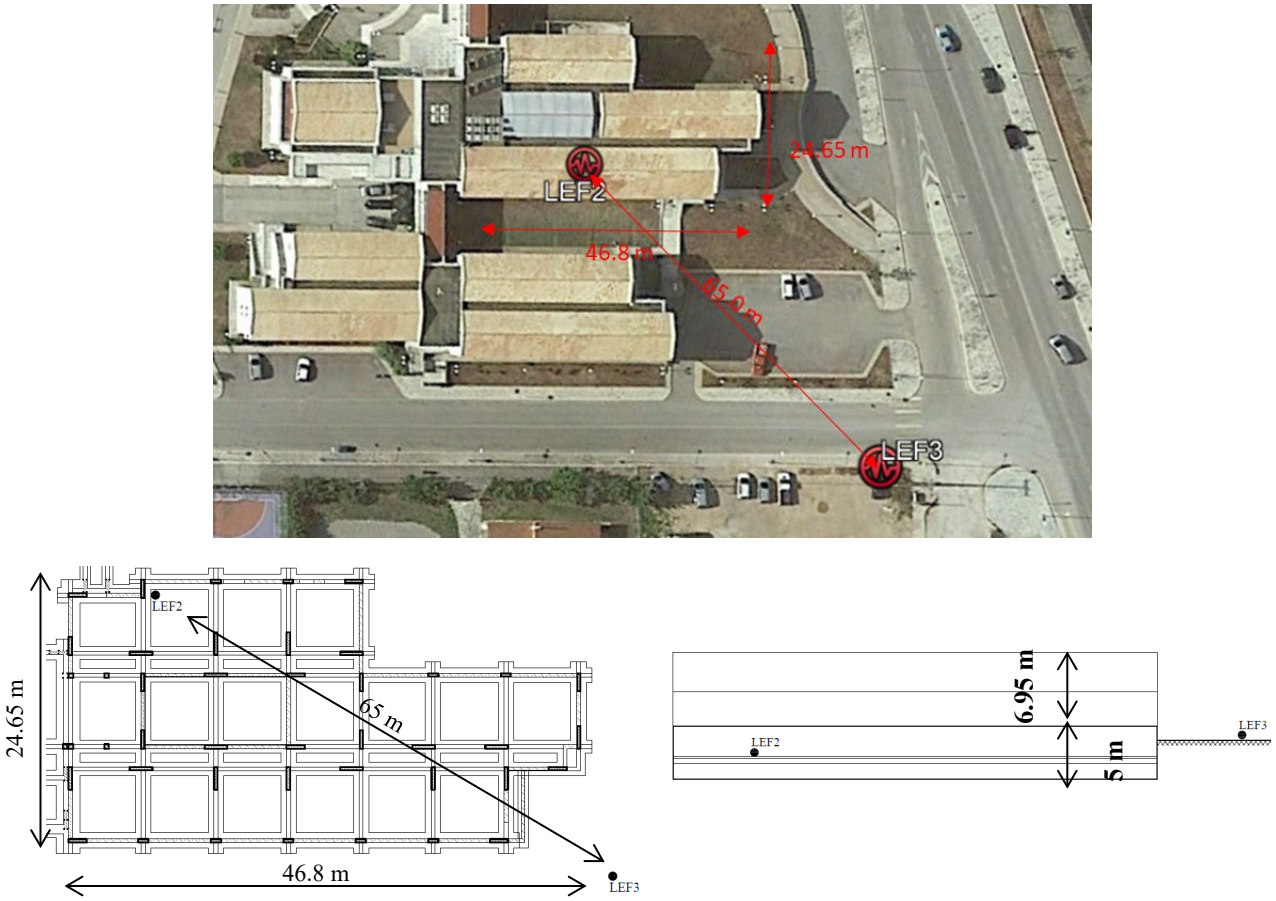

Fig. 3 Plan dimensions of administration building of Lefkada and position of the accelerographic stations (LEF2 and LEF3). Top: top view of site along with building dimensions and relative distance between stations LEF2 and LEF3. Bottom left: plan view of building foundation and corresponding dimensions. Bottom right: schematic elevation of Lefkada's administration building.

2.2.2 Soil profile

Information regarding the soil profile on which this specific structure is founded was taken from downhole measurements, in-situ tests (SPT) and laboratory tests performed at soil samples from a nearby geotechnical borehole (Gazetas et al., 2004). The shear wave velocity profile, as well as, a soil section is presented in Fig. 4. The average shear wave velocity resulting from the upper 30m below grade is calculated equal to $V_{s,30}$= 282m/sec. According to Eurocode 8 site categorization system, the soil profile at Lefkada's administration building site is also classified as type C.

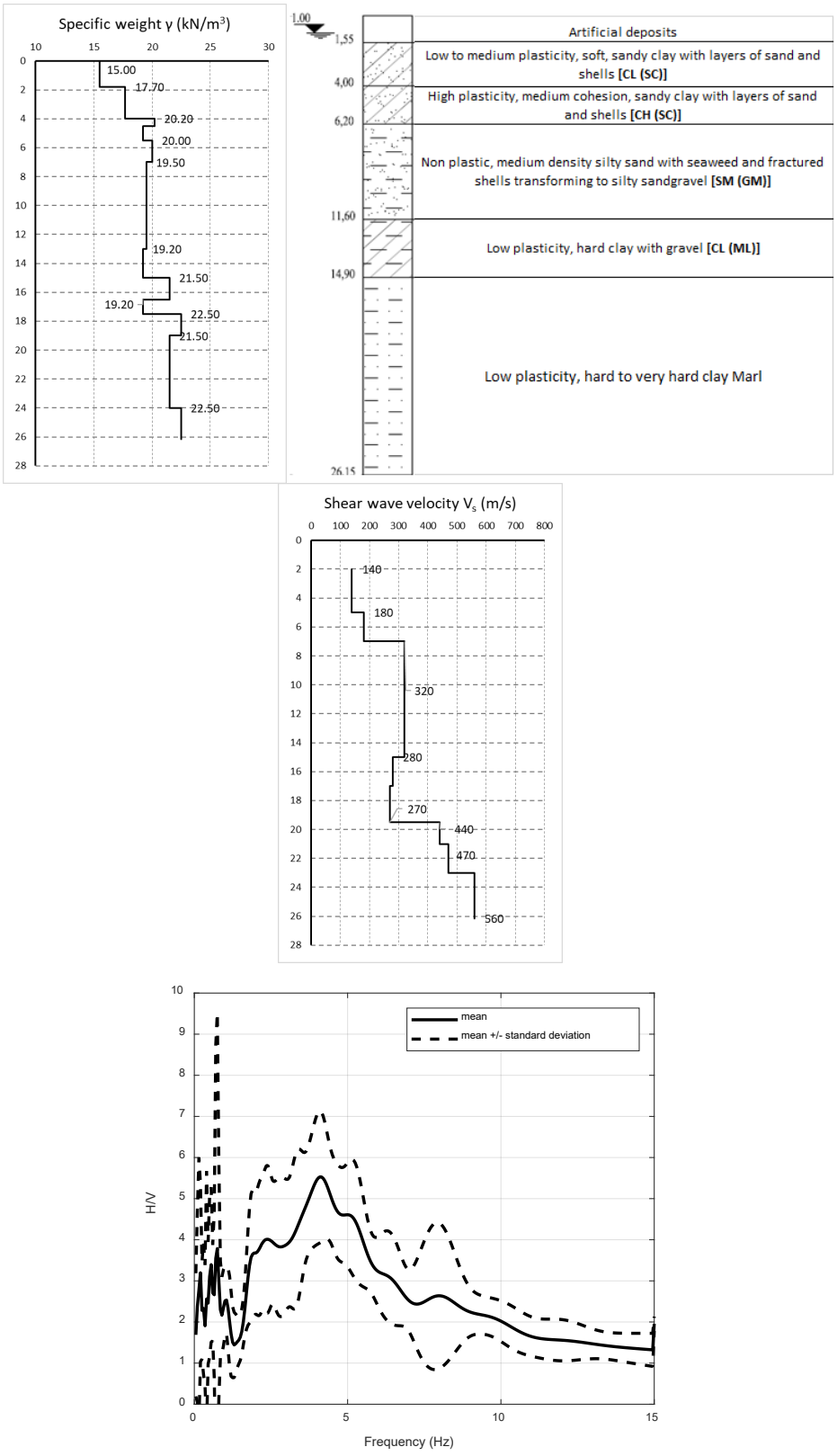

150 **Fig. 4** Top: soil section and shear wave velocity profile at Lefkada's administration building. Bottom: H/V ratio
151 computed through the recordings of the free-field station (LEF3).

3. STRONG GROUND MOTIONS OVERVIEW

3.1 Ground motion sample

Two accelerographic stations have been installed at each of the sites described above, as shown in Figs. 1 and 3. The accelerographs at the stations include 3 components (N–S, E–W and vertical) CMG-5T Guralp type sensors. To assess the influence of SSI on the recorded foundation motion during earthquake excitation, seismic events that were recorded simultaneously both at the free field and inside the building, are examined. A total of 12 and 3 seismic events were recorded at the CO and LAB sites, respectively. Data are provided by the Institute of Engineering Seismology and Earthquake Engineering (EPPO-ITSAK) in Thessaloniki. Date of recording, moment magnitude (M_w), epicentral distance (R_{epi}), hypocenter depth (H) and maximum absolute acceleration between the two horizontal components (PGA) are summarized in Tables 3 and 4. Given that the vertical component was not of interest in this study, only the two horizontal components of the seismic excitation of these events have been considered. However, investigation of the differences between the vertical components of foundation and free-field ground motion may be subject to future research.

Table 3: Seismic Events associated with the recordings at the Cosmos Offices site

#	Day/Month/Year h:min:s	M_w	R_{epi} (km)	H(km)	PGA (cm/s^2)/ direction
1	09/01/2012, 03:22:04	2.8	10.42	0.80	3.5/EW
2	14/02/2012, 01:34:36	5.0	105.04	3.80	1.4/NS
3	12/05/2012, 22:47:55	3.9	12.48	9.40	6.4/NS
4	21/10/2012, 04:43:15	3.3	27.52	9.30	1.4/NS
5	02/07/2013, 10:45:21	4.6	108.05	7.90	0.8/EW
6	03/07/2013, 13:28:21	4.6	108.74	3.70	0.75/EW
7	11/08/2013, 10:23:30	3.6	37.61	4.70	0.9/EW
8	08/09/2013, 10:32:46	3.5	37.56	1.80	0.4/EW
9	11/10/2013, 05:15:32	4.4	38.6	3.80	9.2/NS
10	26/01/2014, 13:56:09	5.9	354	13.50	0.7/EW
11	02/01/2018, 04:24:11	4.7	69.9	13.60	1.8/NS
12	02/01/2018, 17:36:26	4.0	70.27	11.00	0.27/NS

Source: Permanent Regional Seismological Network, Aristotle University of Thessaloniki.

Table 4 Seismic Events associated with the recordings used from Lefkada's administration building site

#	Day/Month/Year h:min:s	M_w	R_{epi}(km)	H(km)	PGA (cm/s^2)/ direction
1	26/01/2014, 13:55:29	5.9	83.57	13.50	38.7/NS
2	17/11/2015, 07:10:07	6.0	23.34	0.00	143.0/NS
3	17/11/2015, 08:33:30	5.1	23.53	7.00	78.0/NS

Source: Permanent Regional Seismological Network, Aristotle University of Thessaloniki.

As shown in the last column of tables 3 and 4, the recordings PGA range indicates that nonlinear soil and structure effects are negligible.

3.2 Ground motion processing

The ground motion recordings were corrected through bandpass filtering so that the signal-to-noise ratio was at least 2. This resulted in low-cut values from 0.05 to 0.1 Hz and in high-cut values from 20-45 Hz. However, the foundation and free-field signals were processed through the same filter so they can be comparable.

In this section, the procedure which was followed is described. The methodology adopted for the calculation of the transfer functions between the foundation and the free-field motion recordings follows from Kim and Stewart (2003) and Mikami et al. (2008). To assess SSI effects on the recorded foundation (i.e., basement) motion, it is essential to

use at least two accelerographic stations, at positions similar to the ones reported for the CO and LAB site. The acceleration time history recorded at the free-field station is defined as $a_{ff}(t)$, whereas the acceleration time history recorded at the basement of the building is defined as $a_{SSI}(t)$. The transfer function between the two recorded motions is defined as the ratio of the Fast Fourier transform (FFT) of $a_{SSI}(t)$, defined as $A_{SSI}(\omega)$, to the FFT of $a_{ff}(t)$, defined as $A_{ff}(\omega)$. According to Kim and Stewart (2003), the transfer function is estimated through transmissibility functions, which are based on the power spectral density (S_{ff} and S_{SSI}) and cross spectral density (S_{ffSSI}) functions. The transmissibility functions $H_i(\omega)$ are defined as:

$$H_1(\omega) = \frac{S_{ffSSI}}{S_{ff}};\ H_2(\omega) = \frac{S_{SSI}}{S_{ffSSI}};\ |H_3(\omega)| = \sqrt{\frac{S_{SSI}}{S_{ff}}} \quad (1)$$

The amplitude of the first two estimates of the transmissibility functions is theoretically equal. However, this is not necessarily verified in practice due to the presence of noise in the two signals or possible nonlinearities at the soil, foundation or superstructure level. $H_1(\omega)$ is less sensitive to the noise of $a_{SSI}(t)$ whereas $H_2(\omega)$ is less sensitive to the noise of $a_{ff}(t)$. The amplitude of $H_3(\omega)$ is intermediate between that of $H_1(\omega)$ and $H_2(\omega)$. The transmissibility function is derived through the coherence function, which is in turn defined according to Pandit (1991) as:

$$\gamma^2(\omega) = \frac{H_1(\omega)}{H_2(\omega)} = \frac{\left|S_{ffSSI}(\omega)\right|^2}{S_{ff}(\omega)S_{SSI}(\omega)} \quad (2)$$

When the coherence function is close to unity, it may be concluded that the noise level is low or effect of non-linearity is limited and that there is a high correlation between the two signals. Reliable estimates of the transfer function can be considered at frequencies where $\gamma^2 \geq 0.8$ (Kim and Stewart, 2003). According to this criterion, Kim and Stewart (2003) reported transfer function estimates based on $H_3(\omega)$ for frequencies up to 10 Hz, since γ^2 decreased significantly for larger frequencies. In this study, the S-wave window of the acceleration time histories was carefully chosen and a time domain smoothing process, proposed in Mikami et al., (2008), was implemented in order to calculate the transfer function through equations (1) and (2). The time domain smoothing includes dividing the acceleration time history into a number of segments while tapering the ends of each sub-segment. Subsequently, the power spectral density function is computed for each tapered portion and then the average of them is calculated to obtain the smoothed spectrum for the whole signal. The procedure parameters for all records were selected to be similar to Kim and Stewart (2003), where 4 non-overlapping sub-segments were used for each signal along with a Kaiser taper. It should be noted that no sensitivity analysis was carried out regarding the smoothing process parameters.

3.3 Transfer functions between the recorded foundation and free-field motions

The process described in section 3.1 was implemented on the available recordings set for both the CO and LAB site so that the transfer function between the foundation and the free-field motion is derived. The process was followed independently in the NS and EW directions. A single transfer function for each site came up as the geometric mean of the average of all available recordings NS and EW transfer functions.

Figs. 5a and 5b present the estimation of transfer functions (STF) for the sites considered using the available recordings for the EW and NS directions, as well as their geometric mean. No significant differences between the transfer functions in the two directions are apparent. The SSI effects on the foundation motion are clearly demonstrated. More specifically, the filtering posed on high frequencies (>2 Hz) by the structure's foundation is evident. At both sites, the transfer functions initiate at amplitude close to unity at zero frequency and degrade up to a specific frequency (about 6 and 4.3 Hz for the CO and LAB site, respectively) to the minimum value of about 0.4 for both sites. After the minimum value is attained, the CO site transfer function remains almost constant, whereas the transfer function of LAB site follows a slightly ascending branch. The former observation is in agreement with the theoretical studies on uniform half-space soil conditions found in the literature (Elsabee etal., 1977; Veletsos et al., 1997; Hossein and Pouran, 2017; Conti et al., 2018). The latter observation may be attributed to oscillations due to reflections of waves initiating from the foundation motion at the interface of soil layers (Luco and Wong, 1987).

Moreover, along with the transfer functions, the uncoupled, translational fundamental frequencies in both principle directions of the structures, calculated in sections 2.1 and 2.2, are shown. It should be noted that the buildings' transverse principal direction is rotated with respect to the North by an angle of 14° and 11° for the CO and the LAB sites, respectively. After rotating the NS-EW system to match the principal directions of the buildings, it was found

that there is not significant error in relating the transverse with the NS direction and the longitudinal with the EW direction. The basic difference between the two sites is the fundamental frequency of vibration with respect to the minimum transfer function value. In particular, the CO building, consisting of reinforced concrete moment resisting frames, is more flexible and consequently, its fundamental frequencies lie below the frequency of the minimum transfer function amplitude. On the other hand, the Lefkada building, consisting of structural walls, exhibits clearly higher fundamental natural frequencies of vibration, compared to the minimum transfer function value. However, this may be of insignificant importance compared to the most pronounced filtering effect which reduces up to 50% the amplitude of the free-field motion at both sites. The *S(ω)* transfer functions exhibit some amplitude fluctuations near the fundamental frequency values indicating the small inertial interaction effect on the foundation motion (Kim and Stewart, 2003). The frequency range shown for each site was determined by the coherence functions calculated per equation (2), shown in figure 6. Beyond the frequency range shown, the transfer functions exhibited intensively jagged shape which along with the low coherence function values indicated high noise levels (Kim and Stewart, 2003). It should be noted that, although relatively high coherence values exist for both sites above 15 Hz, as stated in Kim and Stewart (2003), high frequency ordinates may not be appropriate for comparison to half-space models for kinematic interaction. This type of models is implemented herein as will be shown in the following.

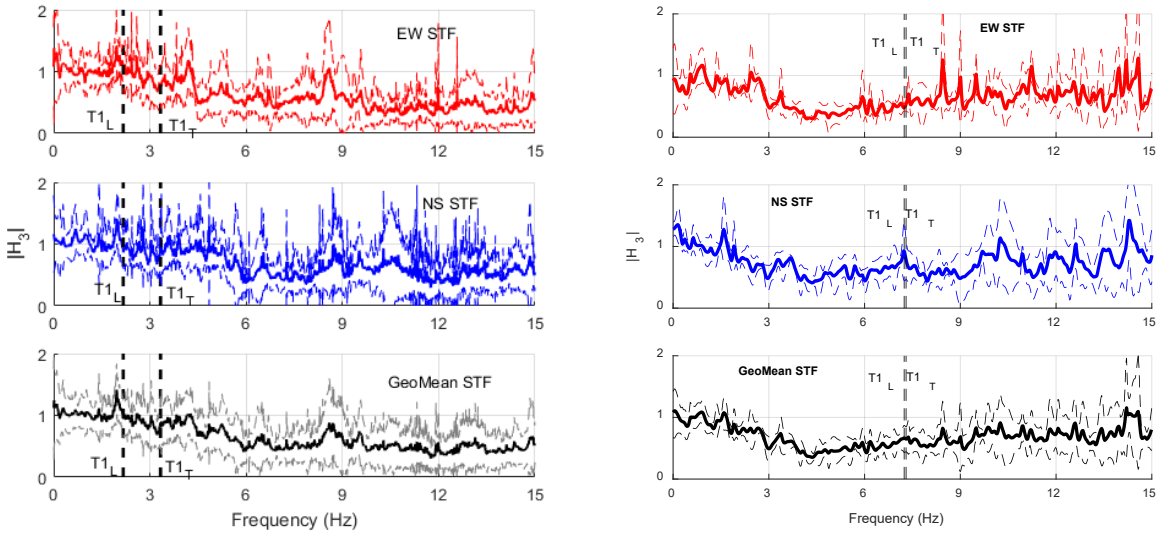

Fig. 5 Estimation of transfer function between the foundation and free field motion for Cosmos Offices (a) and Lefkada's (b) site. The two first rows present the mean and the mean +/- 1 standard deviation transfer functions along the two horizontal components, whereas the last row presents the geometric mean combination of them.

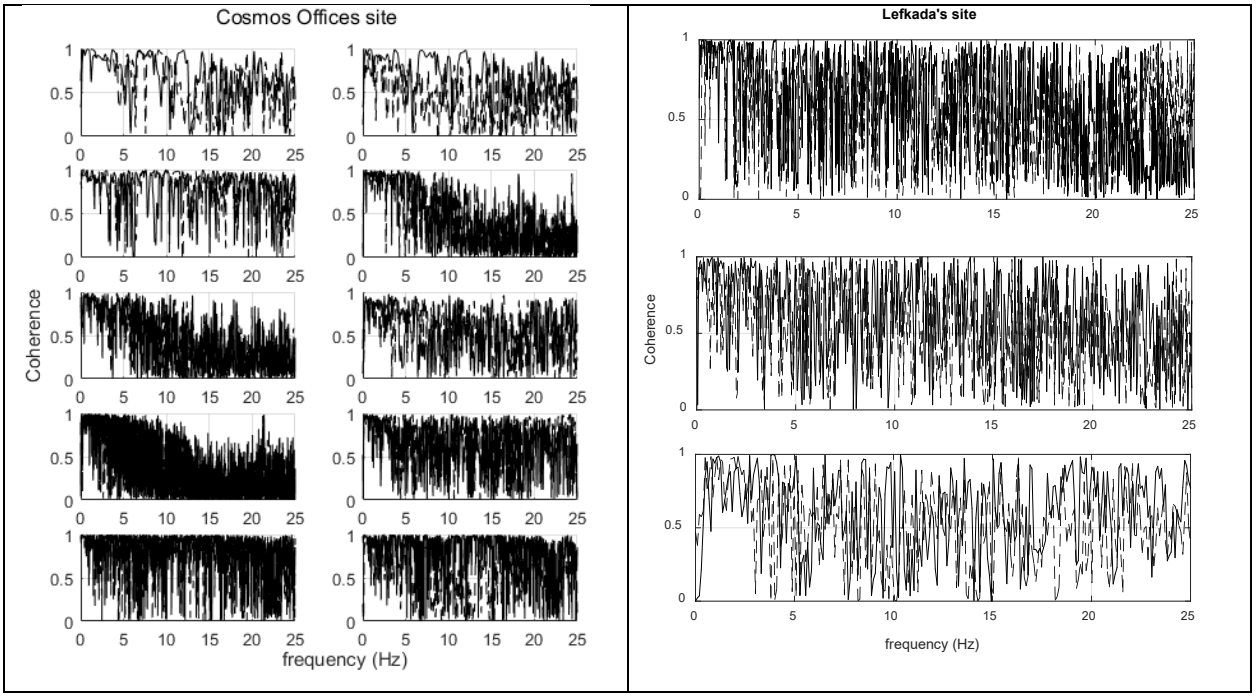

Fig. 6 Coherence functions between foundation and free-field ground motion recordings for CO and LAB sites. The solid and dashed lines correspond to EW and NS components respectively

4. SUBSTRUCTURE ANALYSIS APPROACH

Although the available recordings at stations CO and LAB are a valuable source of information regarding the relationship between the foundation and the free-field motion, their number is not adequate to obtain regression expressions in terms of their intensity and frequency content. Therefore, an analytical procedure is undertaken employing the kinematic and inertial decoupling of the sub-structured soil-foundation-superstructure system for the two sites, utilizing available recordings from the HNAN with the aim to evaluate whether a relationship between the foundation and the free-field motion is indeed feasible. In the following, a brief description of the methodology adopted is given. Subsequently, the applicability of the method is investigated by computing the transfer function analytically and comparing the outcome with the recorded transfer functions shown in section 3. Finally, parametric analyses are performed for the two sites with multiple recordings of the HNAN to develop regression expressions which correlate intensity and frequency content parameters of the two seismically-induced motions within and outside the buildings studied. The available records from the two stations are then used to validate the accuracy of the expressions created**.**

4.1 Description of methodology

The substructure analysis consists one of the most frequently used methods in analyzing SSI problems. As already mentioned, it consists of two successive steps, namely kinematic and inertial interaction, as described in section1. Kim and Stewart (2003) utilized real seismic recordings, both at free-field and in-structure stations, to calibrate the analytical kinematic interaction method of Veletsos et al. (1997), which is related to base slab averaging effects. For in-structure stations located at buildings with embedded foundation, they also used the analytical expressions of Elsabee et al. (1977) that account for foundation embedment effects. The same methodology was implemented herein to account for kinematic interaction effects and is briefly described in the following. The outcome of the kinematic interaction is the Foundation Input Motion (FIM). The transfer function between the FIM and the free-field, ground surface motion due to embedment effects is calculated according to Elsabee et al. (1977) as:

$$|H_{uD}(\omega)| = \begin{cases} \cos\left(\frac{D}{r}a_0\right) a_0 \le 0.7\left(\frac{\pi}{2}\cdot\frac{r}{D}\right) \\ 0.453 \qquad a_0 \ge 0.7\left(\frac{\pi}{2}\cdot\frac{r}{D}\right) \end{cases}, \quad a_0 = \frac{\omega b_e}{V_s} \tag{3a}$$

$$|H_{\Phi D}(\omega)| = \begin{cases} \frac{0.257}{B}\cdot\left(1-\cos\left(\frac{D}{r}a_0\right)\right) a_0 \le \left(\frac{\pi}{2}\cdot\frac{r}{D}\right) \\ \frac{0.257}{B} a_0 \ge \left(\frac{\pi}{2}\cdot\frac{r}{D}\right) \end{cases} \tag{3b}$$

where D is the foundation embedment depth, B the half-width of the foundation, L the half-length of the foundation, V_s the average shear wave velocity along the embedment depth, $r=\sqrt{(A_f/\pi)}$, the equivalent radius of foundation with area and $b_e=\sqrt{(4BL)}$. H_{uD} is the transfer function between the translational components of FIM and free-field motion whereas $H_{\Phi D}$ is the transfer function producing rotational components of FIM as an effect of embedment. The transfer function due to base slab averaging effects (H_{uB}) is calculated based on Veletsos et al. (1997) as:

$$|H_{uB}| = \sqrt{f_1 \cdot g_1} \tag{4a}$$

where:

$$f_1 = B1 - B3 - \frac{e_y}{4d_y^2}\, B2 \tag{4b}$$

$$B1 = \frac{\sqrt{\pi}}{2d_y}\exp\left(-\frac{{e_y}^2}{4{d_y}^2}\right) R\left[\Phi\left(2d_y + i\frac{e_y}{2d_y}\right)\right] \tag{4c}$$

$$B2 = \frac{\sqrt{\pi}}{2d_y}\exp\left(-\frac{{e_y}^2}{4{d_y}^2}\right) I\left[\Phi\left(2d_y + i\frac{e_y}{2d_y}\right) - \Phi\left(i\frac{e_y}{2d_y}\right)\right] \tag{4d}$$

$$B3 = \frac{\left(1-\exp\left(-4d_y^2\right)\cos\left(2e_y\right)\right)}{4d_y^2} \tag{4e}$$

$$g_1 = \frac{\sqrt{\pi}}{2d_x}\,\Phi(2d_x) - \frac{1-\exp(-4d_x^2)}{4d_x^2} \tag{4f}$$

$$e_y = \sin(a_v)\cdot\omega\cdot\frac{B}{V_s} \tag{4g}$$

$$d_y = \frac{\gamma_y \omega B}{V_s} \tag{4h}$$

$$d_x = \frac{\gamma_x \omega L}{V_s} \tag{4i}$$

$$\Phi(x) = \frac{2}{\sqrt{\pi}}\int_0^x \exp(-u^2)\, du \tag{4j}$$

In equation (4g), a_v is the incidence angle of the seismic waves with respect to the vertical direction, which was considered as zero herein, Φ(x) is the error function and γ_x and γ_y are wave incoherence parameters. Kim and Stewart (2003) calibrated the wave incoherence parameters to their records data and suggested expression (5). The dependence of κ_a on the surface geology has been discussed from others as well (Luco and Wong (1986); Somerville et al. (1991) pointing out that it is higher for stiff soil or rock sites than young alluvium sites. However Kim and Stewart (2003) calibrated it to a large set of both foundation and free-field recordings data. Thus, the index "a" in κ_a denotes the apparent wave incoherence data as instead of wave incoherence, includes foundation flexibility and wave inclination with respect to the vertical. Expression (5) is adopted herein due to lack of sufficient number of data in Greece to develop a region-specific relationship.

$$\kappa_\alpha = \gamma_x = \gamma_y = 7.4 \cdot 10^{-4}(V_s - 50) \quad (5)$$

The FIM is further modified by inertial interaction analysis that involves two steps. At first, the foundation frequency-dependent impedance functions of the degrees of freedom of interest are calculated. The real part of the impedance functions represents soil stiffness whereas the imaginary part expresses the soil damping due to radiation and inelastic response. In the study presented herein, the impedance functions were calculated according to the analytical expressions of Pais and Kausel (1988) which refer to uniform half-space soil conditions. The shear wave velocity introduced in the impedance function analytical expressions is V_{szp}, which is defined as the average value of V_s along a depth of z_p (Stewart et al. (2003):

$$z_p = 0.75\sqrt{A_f/\pi}, \qquad horizontal\ translation \quad (6a)$$

$$z_p = 0.75\sqrt{4I_f/\pi}, \qquad rotation\ about\ horizontal\ axis \quad (6b)$$

where I_f is the moment of inertia of the foundation footprint about the corresponding horizontal axis.

Subsequently, the dynamic analysis of a system consisting of the superstructure supported by the foundation and the surrounding soil, represented by the foundation impedance functions, is performed. In analyses reported herein, superstructure is modelled as an equivalent single degree of freedom (SDOF) system, as shown in Fig. 6. Thus, the analysis is two-dimensional and only the horizontal translations and rocking degrees of freedom of the foundation are considered. The equations of motion of the system shown in Fig. 6 are the following.

$$\widetilde{K_x}(U_o - U_G) + \widetilde{K_{x-ry}}(\Phi_o - \Phi_G) = \omega^2[m_0 U_o + m_1(U_o + H_c\Phi_o + U_1)] \quad (7a)$$

$$\widetilde{K_{x-ry}}(U_o - U_G) + \widetilde{K_{ry}}(\Phi_o - \Phi_G) = \omega^2[I_0\Phi_o + I_1\Phi_o + m_1 H_c(U_o + H_c\Phi_o + U_1)] \quad (7b)$$

$$-m_1\omega^2(U_o + H_c\Phi_o + U_1) + \widetilde{K_{str}}U_1 = 0 \quad (7c)$$

where U_0 is the translational response of the foundation, U_G the horizontal component of the FIM, Φ_0 the rocking response of the foundation, Φ_G the rotational component of the FIM and $U_1$the response of the superstructure. The damping ratio of the superstructure is taken as 5% as is the case in common practice and SSI analyses met in literature (e.g. Mylonakis et al., 2006). The $\widetilde{K_i}$ terms correspond to the complex impedance functions of the foundation where the real part expresses soil stiffness and the imaginary part stands for damping. According to the nomenclature of Fig. 7, the relationship is sought between the coupled response of the foundation (U_0 and Φ_0) with the free-field motion.

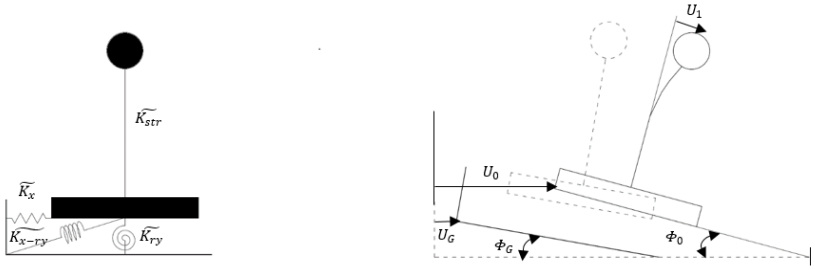

Fig. 7 System to be analyzed at the final step of SSI analysis (adapted from Mylonakis et al., 2006)

4.2 Comparison between analytical and recorded transfer functions

At first, the substructure analysis approach, described in section 4.1, was implemented for the estimation of the transfer function between the foundation and the free-field motion for the sites considered. It should be noted that, given the low intensities of the events examined, the soil was assumed linear elastic and small strain soil properties were used, without any reduction of shear modules G_0 and the subsequent values of V_s required in eq. 3a, 3b, 4h and 4i. Analysis

was performed for each site (CO and LAB), independently in their principal directions (longitudinal and transverse), thus, two transfer functions were obtained. The final transfer function for each site was computed as the geometric mean of the longitudinal and transverse transfer functions since the effect of the superstructure response in the two horizontal directions on the foundation motion is limited to a narrow range of frequencies around the fundamental one (Kim and Stewart (2003), Mylonakis et al. (2006)).

Figs. 8(a, b) present the estimates of the transfer functions between the in-building and the free-field motion for the two sites and their comparison with the recorded ones. Two analytical transfer functions are presented for each case. The dashed curve corresponds to the transfer function consisting only of the translational component of the foundation response (U_0). The solid curve includes both the translational and the rocking component of the foundation motion (U_0 and Φ_0). The rocking component was included because the accelerograph inside the building is not located at the base of the foundation but at the basement floor which is approximately 1.5m and 2.0 m above the foundation base for the CO and the LAB site respectively. Thus, the displacement attributed to possible rocking of the foundation was considered as the product of the Φ_0 and the distance between the basement floor and the foundation base.

Examining Fig. 8 it is seen that the analytical transfer functions capture, at least on average, reasonably well the ones derived directly through the recorded ground motions. For the case of the CO building, the analytical approach shows very good agreement across almost all frequencies except for the range of 3–5Hz and 8-9Hz. It is also observed that matching improves when the rocking component of the foundation motion is considered. For the LAB site the matching is also quite good up to 5Hz above which the recorded TF follows an ascending branch which cannot be captured by the substructure analysis approach implemented herein. It is also observed that values of the analytical transfer function are larger than those of the experimental one for frequencies 2-4 Hz. Overall, given the simplicity of the analytical method and the complexity of the phenomena taking place, the matching between the analytical transfer functions and the ones derived directly through the recorded ground motions is deemed satisfactory. This builds confidence for using the above approach to populate the sample of ground motions and seek specific trends, in terms of frequency content and amplitude, between the free-field ground motions and those recorded with an instrumented building.

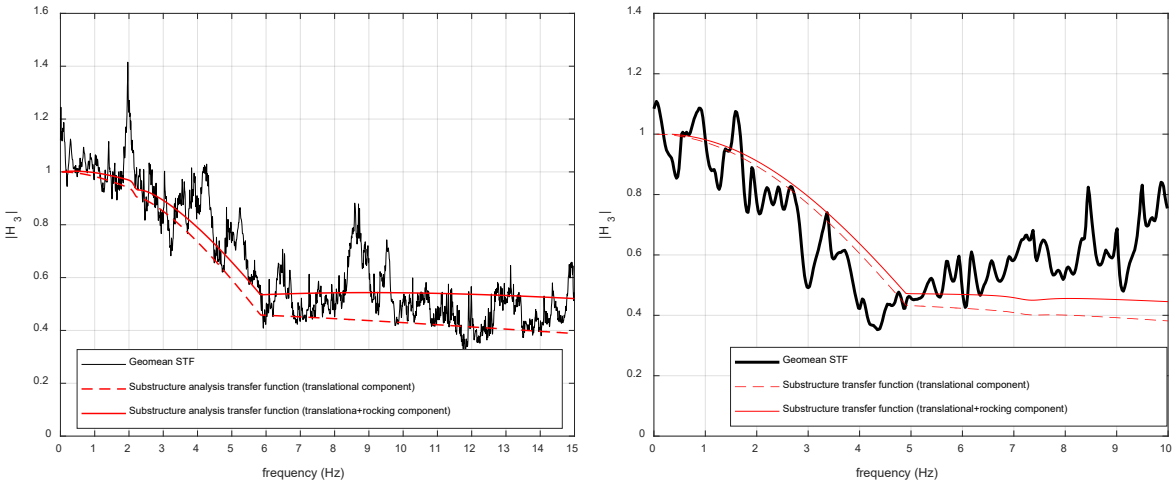

(a) **(b)**

Fig. 8 Estimation of transfer function through substructure analysis and comparison with recordings transfer function: Cosmos Offices (a) and Lefkada Administrative Building (b)

5. PARAMETRIC ANALYSIS

5.1 Strong motion recordings

In this section, the parametric substructure SSI analysis scheme is presented. Note that the structure, as well as the soil properties of the two sites are considered known and kept constant whereas the seismic input excitation is varied by using motions recorded at the outcrop or over stiff soil profiles that can be classified as of type A according to

Eurocode 8 (EN1998-1). Ground motions were then applied at the bedrock level of the CO and LAB soil profiles and a 1D, equivalently linear, site response analysis was performed for all motions. Information on the seismic events chosen is given in Table 5 while Fig. 9 presents the PGA, root mean square acceleration (a_{rms}) and Arias Intensity (Ia) with respect to the mean period (T_m) of the motions. The two horizontal components of the seismic recordings were used independently in the parametric analyses.

Table 5 Information of seismic events and stations chosen for the parametric analyses

#	Event	M_w	Station Code	$V_{s,30}$ (m/s)	Source	PGA (cm/sec^2)
1	18/02/1986	4.8	THE2	965.0	EPPO-ITSAK	8.60
2	18/05/1988	5.3	VLSA	872.0	NOA	83.0
3	22/05/1988	5.4	VLSA	872.0	NOA	83.0
4	13/02/1995	4.8	THE2	965.0	EPPO-ITSAK	4.80
5	03/10/1999	4.0	ATH4	1020.0	EPPO-ITSAK	9.20
6	07/09/1999	5.9	ATH4	1020.0	EPPO-ITSAK	118.6
7	07/09/1999	-	ATH4	1020.0	EPPO-ITSAK	27.50
8	23/11/2011	3.7	ZKRA	877.0	NOA	0.40
9	26/01/2012	4.1	ZKRA	877.0	NOA	1.04
10	27/01/2012	5.3	ZKRA	877.0	NOA	0.80
11	10/06/2012	5.9	ZKRA	877.0	NOA	0.80
12	12/09/2012	5.2	ZKRA	877.0	NOA	0.36
13	06/04/2013	5.1	ZKRA	877.0	NOA	0.26
14	15/06/2013	5.6	ZKRA	877.0	NOA	1.60
15	16/06/2013	5.7	ZKRA	877.0	NOA	1.10
16	09/08/2013	4.7	VSK1	1183.0	EPPO-ITSAK	0.11
17	16/09/2013	4.9	VSK1	1183.0	EPPO-ITSAK	0.12
18	11/01/2014	4.7	VSK1	1183.0	EPPO-ITSAK	0.60
19	26/01/2014	5.9	VSK1	1183.0	EPPO-ITSAK	96.8
20	26/01/2014	5.3	VSK1	1183.0	EPPO-ITSAK	25.0
21	03/02/2014	5.8	VSK1	1183.0	EPPO-ITSAK	57.0
22	22/08/2014	5.0	VSK1	1183.0	EPPO-ITSAK	0.06
23	24/10/2014	5.2	VSK1	1183.0	EPPO-ITSAK	1.71
24	08/11/2014	5.1	VSK1	1183.0	EPPO-ITSAK	11.6
25	08/11/2014	5.1	VLSA	872.0	NOA	257.0
26	17/11/2014	5.2	VSK1	1183.0	EPPO-ITSAK	0.14
27	17/11/2014	5.3	VSK1	1183.0	EPPO-ITSAK	0.09
28	28/01/2015	5.0	ZKRA	877.0	NOA	0.20
29	16/04/2015	6.1	ZKRA	877.0	NOA	56.0

30	17/04/2015	5.3	ZKRA	877.0	NOA	11.0
31	09/06/2015	5.1	VSK1	1183.0	EPPO-ITSAK	0.08
32	09/06/2015	5.3	ZKRA	877.0	NOA	11.0
33	13/01/2009	4.4	THE2	965.0	EPPO-ITSAK	0.16

Source: Permanent Regional Seismological Network, Aristotle University of Thessaloniki.

5.2 Analysis process

The free-field seismic ground motion, as well as the effective soil properties (V_s and damping) were derived from each site response analysis. Then, considering the foundation properties of each site, implementation of the kinematic interaction process followed eq. (3) and (4) to obtain the FIM at the base of the foundation. Subsequently, based on the soil profile effective properties and the characteristics of the foundation, the impedance functions of eq. (6) were calculated (Pais and Kausel, 1988). Finally, a frequency domain dynamic analysis of the system was performed and the total response of the foundation in terms of the translation and rotation motion U_0 and Φ_0 was derived thus leading to a superstructure supported by springs with properties defined by the impedance functions and excited by the FIM. The uncertainty associated with shear wave velocity profile was also taken into consideration for both sites. The rationale behind this decision is the fact that ground motion amplification in non-uniform soil profiles is strongly affected by the shear wave velocity contrast between successive layers as well as the bottom layer and the (elastic or rigid) bedrock. The varied V_s profile samples were realized through the computer program Strata (Kottke et al, 2013), which incorporates the models developed by Toro (1995). The latter is an improvement of previous efforts and correlates soil layers through proposed parameters depending on the soil category. The shear wave velocity at the mid-depth of a layer is assumed to follow a log-normal distribution, while the median V_s values are taken based on the information given in section 2.

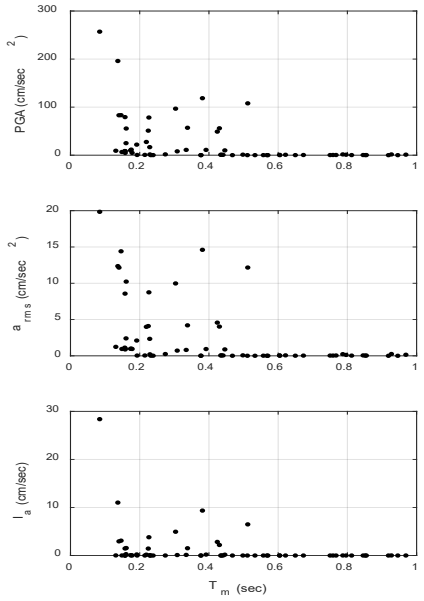

Fig. 9 Main characteristics of outcrop bedrock motions used in the parametric analyses process.

Minimum and maximum values were set, based on available downhole test results (Gazetas et al., 2004). In total, 400 random shear wave velocity profiles were developed for every site. The number of 400 random profiles results from previous experience on this matter where mean value and standard deviation are stabilized when the number of random profiles is at least 400. Ultimately, the mean μ and standard deviation $\pm 1\sigma$ values of the shear wave velocity profiles were considered in the subsequent SSI analyses along with the corresponding damping levels and the free-field ground surface response. It should be noted that this process was repeated for each of the input earthquake excitations reported in table 5. The depth to bedrock varied from 50 to 150m for the CO site, based on the soil sections presented in

Manakou et al. (2008) and the authors' judgment. On the other hand, the depth to bedrock for the LAB site varied from 50 to 70m. The difference between the two sites' depth to bedrock variability is based on the uncertainty associated with it, which is much higher in the case of the CO site. Moreover, the shear modulus reduction and damping curves of Darendeli (2001) and Idriss (1990) where implemented in Strata based on available information, in order to obtain the effective properties (effective shear modulus and damping ratio) for each layer.

5.3 Parameters investigated

Several alternative velocity- or acceleration-based intensity measures (IM) exist, however, the first are in principle related to high frequencies of motions, which is the frequency range within which kinematic SSI effects are more pronounced. Thus, acceleration-based intensity parameters were regarded as most suitable in expressing the SSI effect on the foundation motion. The IMs chosen herein are: peak ground acceleration (PGA), acceleration root mean square (a_{rms}) (Kramer, 1996) and Arias Intensity (I_A) (Arias, 1970). All three of them were found to correlate well with frequency content parameters. The a_{rms} and I_A are calculated as shown in eq. (8) and (9), respectively. In these equations, *a(t)* is the acceleration time history, T_d is the duration of the signal and *g* is the acceleration of gravity.

$$a_{rms} = \sqrt{\frac{1}{T_d}\int_0^{T_d} [a(t)]^2 dt}. \quad (8)$$

$$I_A = \frac{\pi}{2g}\int_0^{T_d} a(t)^2\, dt. \quad (9)$$

A few single-valued frequency content parameters of strong motions were investigated, such as the predominant period T_p of the ground motion, the ratio of peak velocity to peak acceleration v_{max}/a_{max} and the mean period T_m, as defined by Rathje et al. (1998). The latter exhibited the best correlation with the preceding IMs. Note that the mean period T_m is defined as shown in eq. (10) where C_i is the ordinate of the Fourier amplitude spectrum at every frequency f_i. The frequency range considered was between 0.25 and 20 Hz (Rathje et al. (1998)), equally distributed on a linear scale.

$$T_m = \frac{\sum C_i^2/f_i}{\sum {C_i}^2}, \qquad 0.25\ Hz \le f_i \le 20\ Hz \quad (10)$$

5.4 Regression analysis and comparison with recorded data

After the analysis was completed for each seismic excitation input, the ground motion intensity and frequency content parameters were calculated for both, free-field and foundation motions. Then, the ratios of the intensity measure of the foundation to that of the free-field motion was plotted against the frequency content parameter. Regression analysis followed with the aim to extract an analytical relationship.

Fig. 10 presents parametric analysis results for the CO site. The red, solid line corresponds to the mean analytical expression fitted to analysis results, whereas the red dashed lines correspond to the $\pm\sigma$ fitted expressions. The recorded data of the CO site are also presented for comparison. At the vertical axes of the graphs, the ratio of foundation motion IM to the one of free-field motion is plotted. Two frequency content parameters are reported at the horizontal axes of the figure. First, T_{mff} corresponds to the mean period of the free-field acceleration time history while T_{mfnd} is the mean period of the acceleration response time history of the foundation. It is noteworthy that both mean periods correlate well with intensity parameters ratios as the R^2 factor is close to unity. T_{mff} seems to correlate slightly better than T_{mfnd} whereas the a_{rms} ratio provides analytical expressions with higher R^2. The IM ratio starts from a minimum value near 0.4 and increases as the mean period of the seismic motion (either foundation or free-field) increases. This is a clear indication that the reduction of the intensity at the foundation level, compared to free-field, is more pronounced for motions rich in high frequency content (i.e., low T_m) and becomes negligible for low frequency motions. Such a trend is in accordance with the kinematic interaction effect illustrated by the transfer functions described in Section 4.1, as well as with the recorded transfer function reported in Section 3. It should be noted that the PGA ratio values at low mean periods present significant scattering. Such values of periods may come up from recordings of earthquake events which are either close to the station or/and they exhibit low magnitude. Based on the intensity of the recordings data of the CO site (table 3) it may be inferred that the scattering presented is affected by the presence of noise. However, when the a_{rms} is considered as IM, the scattering within the whole mean period range seems to be significantlyreduced, providing thus clear trends regarding the relationship between T_{mff} or T_{mfnd} and the IM ratio of the two motions.

Similar trends are observed in Fig. 11, where parametric analysis results of LAB site are presented. Notably, the regression analysis coefficients are larger than the ones of the CO site by about 27% in terms of log(x) when T_{mff} is used as the frequency content parameter. Furthermore, when T_{mfnd} is used, are larger than the ones of the CO site by about 19% in terms of log(x). This does not stand for the I_A ratio expressions which are very close to the ones of the CO site.

Since ground motions recorded at accelerographic stations inside the building and at the free-field, are available for both sites, verification of the accuracy of the methods implemented herein is possible. The available recordings at the CO site lead to a sample of IM ratios for a wide range of mean periods (0.1 to 1.2 sec). The recordings data expressing PGA ratio as a function of T_{mff} presents significant scattering, especially for low mean period values (0.1- 0.2 sec). This scattering cannot be captured adequately by the substructure analysis method implemented herein. However, for larger mean period values, recording data lie around the mean fitted to the analysis data curve. On the other hand, at LAB site, the mean period range, for which real recording intensity parameter ratios exist, is limited. This is evident in Fig. 11 where only 6 records-based IM ratio points exist, all for mean periods above 0.42sec, hence, meaningful comparison is not feasible.

When considering the results for the a_{rms} ratio (Fig. 10 and 11, middle, for CO and LAB sites, respectively) the fitted curves present significantly improved matching as quantified by the increased R^2. Again, at low mean period values, the actual record-based, a_{rms} ratios are higher than those predicted analytically. However, the trend observed by the recorded data is similar to the analytical predictions. For larger mean period values, the recordings data a_{rms} ratio values lie around and close to the mean fitted to the analysis data. The observations made for the a_{rms} expressions stand for the I_A ratios as well (Fig. 10 and 11, bottom, for CO and LAB sites, respectively).

It is noted that some of the LAB site data fall below the analytical expression mean curve. This may be the result of the equivalent linear approximation for the soil non-linear site response, instead of a fully non-linear analysis.

Figs. 12 – 14 further present the relationship between PGA, a_{rms} and I_A ratios and the mean period of the free-field motion, respectively, including all the available data of the examined sites (analysis and recordings) in a single sample. This was deemed feasible due to similarity between the soil profiles of the CO and LAB sites and the fact that the effect of the superstructure response affects the foundation response only in a limited range of frequencies around the structure's fundamental frequency (Kim and Stewart, 2003). Also, the foundation footprint area of the two buildings, which strongly affects base-slab averaging, differs only by about 18%. This difference was deemed insignificant for now, believing that the foundation embedment effect is of higher importance. However, such assumption needs to be further investigated. Fig. 12 shows that data fit curve on the parametric analysis data exhibits a high R^2 factor but deviates significantly from the corresponding fitted curve derived using the actual records. More specifically, 50% of the PGA ratios derived with the recorded do fall within the mean $\pm 1\sigma$ range of the parametric analysis data fit, however, the data fit of the recorded data has such a low R^2 factor (0.082), that the two samples (analytical vs. recorded) cannot be reliably compared. This is a clear indication that no relationship can be established between PGA ratio and T_{mff} based on the available data.

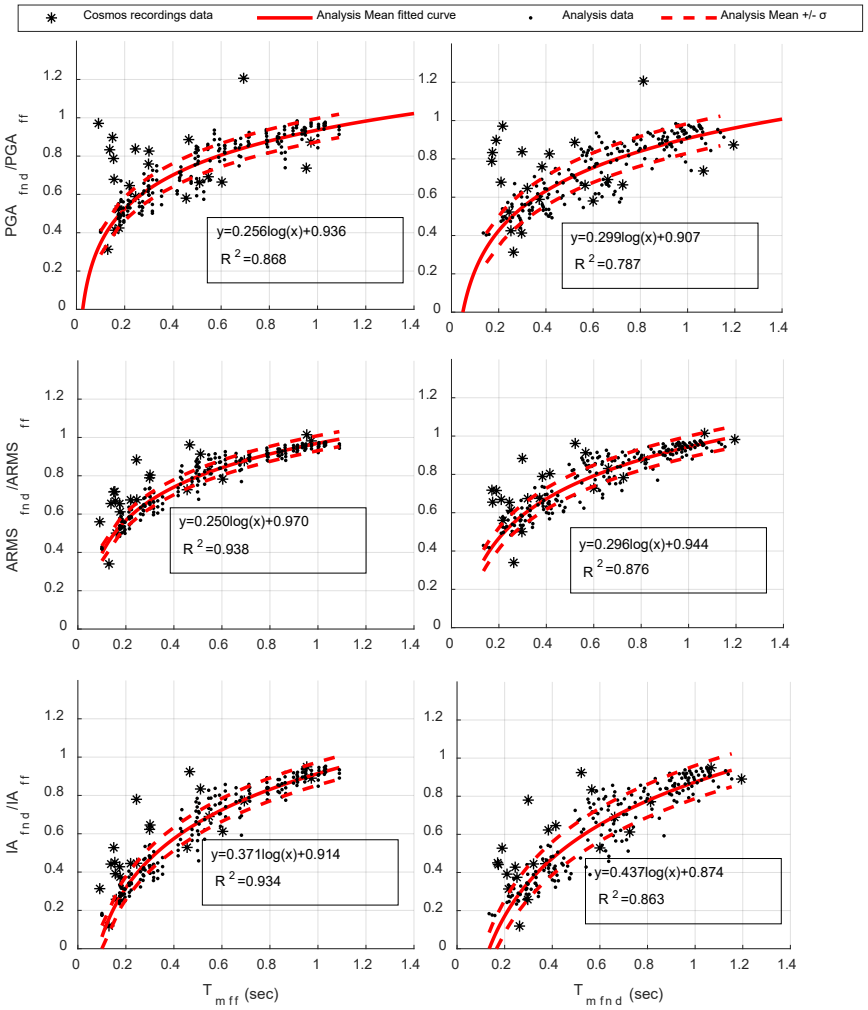

460

461 **Fig. 10** Parametric analysis results for the Cosmos Offices site. T_{mff} and T_{mfnd} represent the mean period of the free-
462 field and foundation motion respectively

463

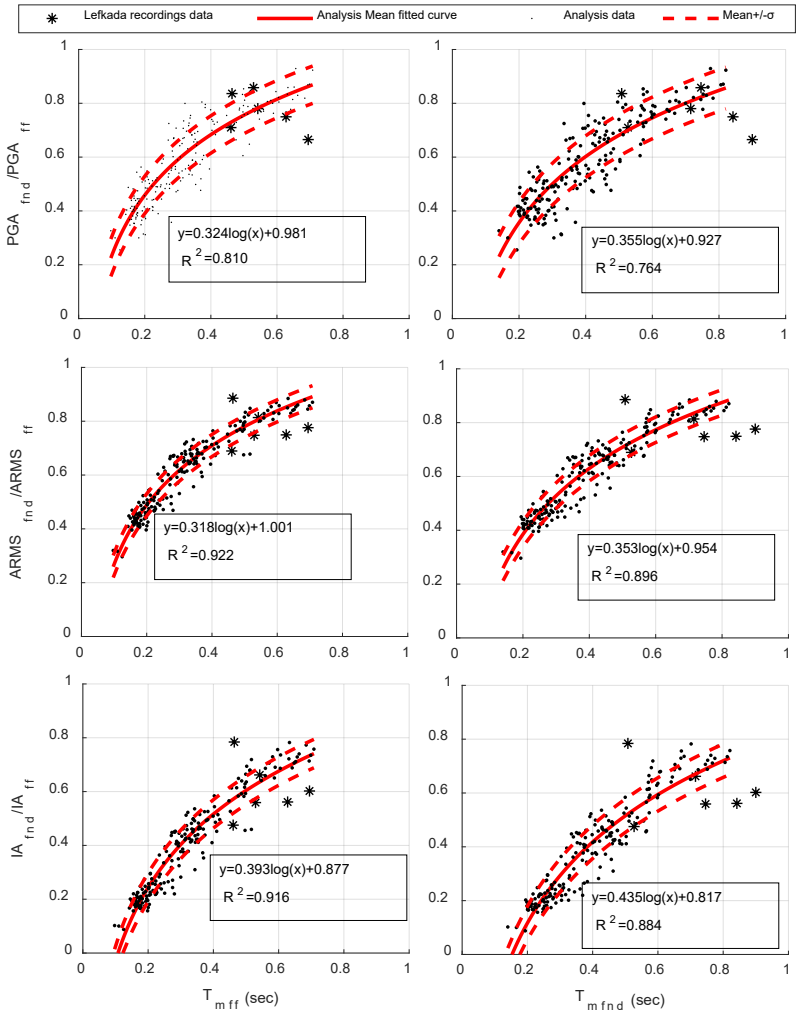

Fig. 11 Parametric analyses results for the Lefkada Administration Building. T_{mff} and T_{mfnd} represent the mean period of the free-field and foundation motion respectively

Contrary to Fig. 12, when the a_{rms} is used as the IM of interest, the R^2 factor is improved being reaching 0.925 for the analytical predictions and 0.52 for the recorded data. The most pronounced difference, however, between the analysis and recorded data fit expressions (except for the R^2 factor) is the inclination of the curve, that is, the factor of the log(x) term, which varies by 70%. This difference may be attributed to the smooth transfer function implemented in the analytical sub-structuring approach to consider the kinematic interaction effects (see Fig. 8).

Fig. 14 further presents the wider sample formed for both CO and LAB sites using I_A ratio as the IM of interest and being again plotted as a function of the mean period T_{mff} of the free-field ground motion. The situation resembles to the case of a_{rms} ratio as per the R^2 factor of the analysis and recordings data fit curves. It is important to note that the variable coefficient of the analysis data fit expression is larger than the one of the recordings data by as much as it was for the a_{rms} case (70%). Overall it can be concluded that when the ratio of the intensities of the ground motion at the basement of a building and the free-field is expressed in terms of a_{rms} or I_A, the analytical solution of kinematic and inertial sub-structuring is reasonably accurate in predicting (and correcting) the intensity ratio between the two locations (inside and outside the instrumented building). It also shows that for mean ground motion periods smaller than 0.5sec, which refers to high frequency and/or near field motions, this difference is far from negligible, varies from 0.2 to 0.8 and should be taken into consideration.

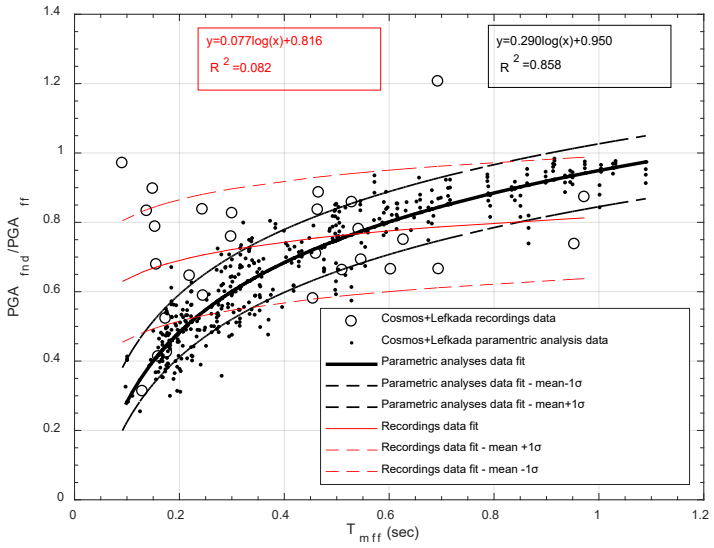

Fig. 12 Relation between PGA ratio and mean period of free field motion of all available data

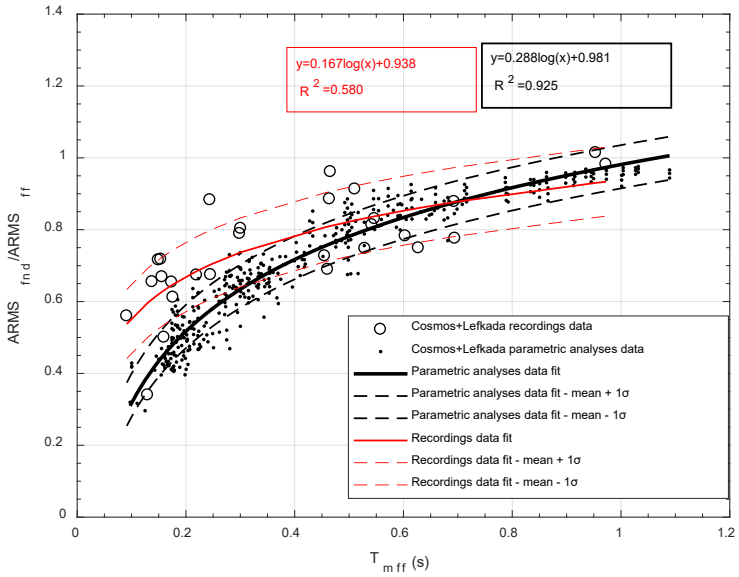

Fig. 13 Relation between a_{rms} ratio and mean period of free field motion of all available data

At this point, it should be noted that normalization of T_{mff} to the fundamental structural period ($T_{0,struct}$) of the sites and to T_{mfnd} were investigated in order to improve the resemblance between the analysis and recordings data and the R^2 factor of the produced relationships shown in figures 11-14. Normalization to $T_{0,struct}$ was made in an attempt to eliminate the effect of superstructure's response. On the other hand, normalization to T_{mfnd} was attempted as T_{mff}/T_{mfnd} could express the filtering effect of the foundation. However, the normalization schemes did not meet any of these expectations. Perhaps, utilization of more recordings data, from multiple sites, may prove these normalization schemes more efficient.

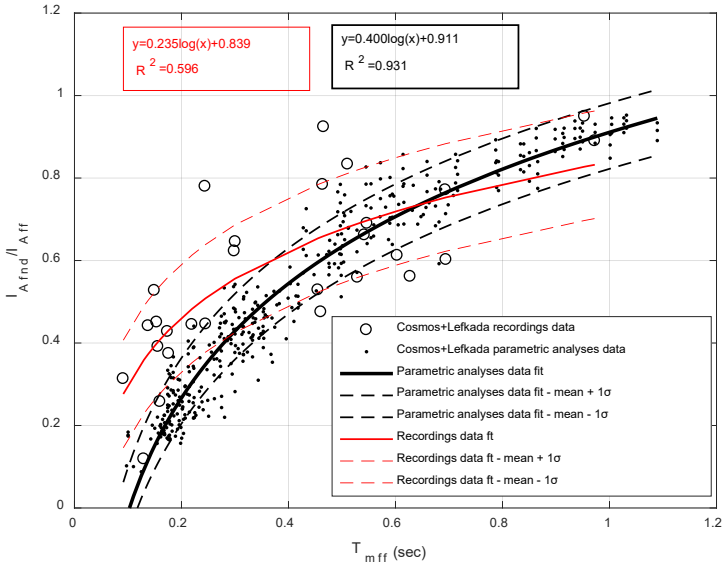

Fig. 14: Relationship between Arias intensity ratio and mean period of free field motion including all available data

Figs. 15 – 17 further present the direct relationship between the intensity measures of the free-field ground motion and that at the foundation level. It is noteworthy that the recorded data indicate a linear relationship between them with an exceptionally high R^2 factor (0.914/0.992, 0.919/0.991 and 0.724/0.993 for the recorded ratios and the analytical predictions and for the PGA, a_{rms} and I_A, respectively). As anticipated, the free-field IM is always larger than the corresponding value of the foundation motion by 49%, 70% and 73% for the three studied IMs. Apart from the generally low dispersion observed, it is interesting to note the excellent matching of the prediction of the SSI effects by means of the analytical solution when the comparison is based on a_{rms}-based linear expressions (Fig. 16). Such a prediction is not equally successful when PGA and I_A are used as IM (Figs. 15 and 17).

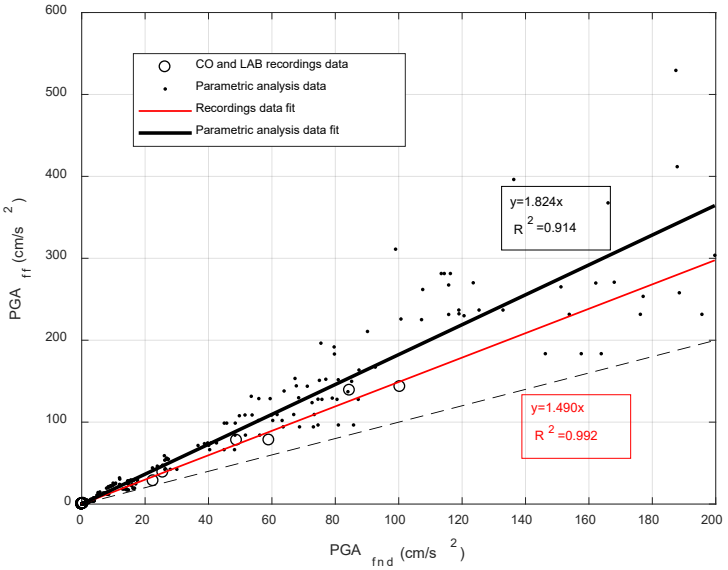

Fig. 15 Relationship between the peak acceleration of free-field and foundation motions

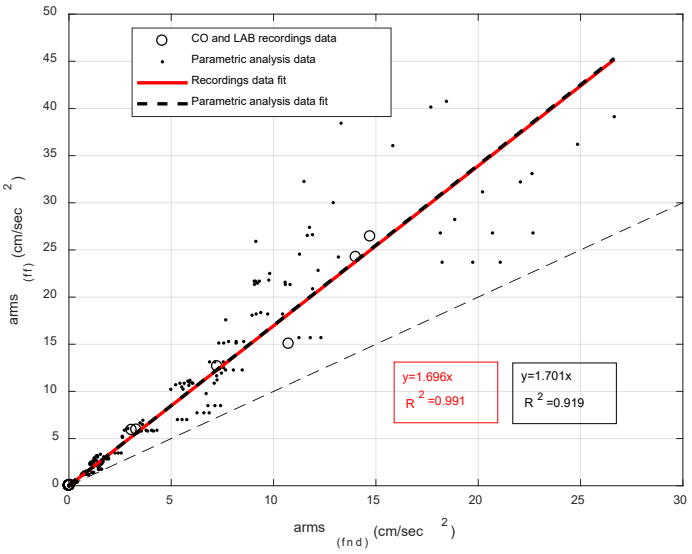

506

507 **Fig. 16** Relationship between the root mean square acceleration (a_{rms}) of free-field and foundation motions

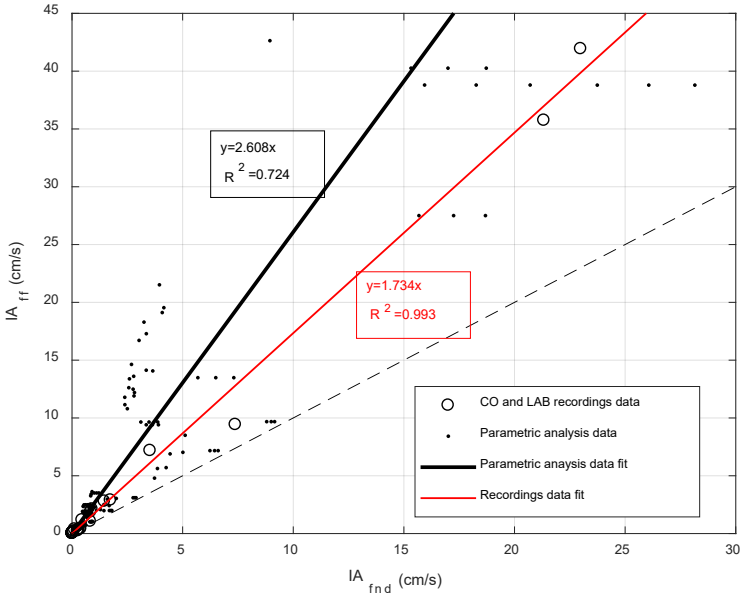

508

509 **Fig. 17** Relationship between the Arias Intensity of free-field and foundation motions

510 Another interesting issue that emerges from Figs. 12-14 is that the discrepancy between the analysis data fit
511 expressions and the recordings data seem to be more important for low mean period values (high frequencies). This
512 may be due to the high frequency flat region of the transfer function between the foundation and the free-field motion
513 (equation 3 and Fig. 8) that was implemented in the parametric analyses. This could also be the reason behind the
514 differences between analysis and recordings data shown in Figs. 15 -17. Furthermore, the parametric analysis data
515 denote that as the intensity of the motions increase, the scattering around the linear fit increases as well. Collection of
516 more recordings data, as well as, investigation of more sophisticated analysis methods is necessary to obtain more
517 rigorous predictions of the effect of SSI on the motions recorded within instrumented buildings.

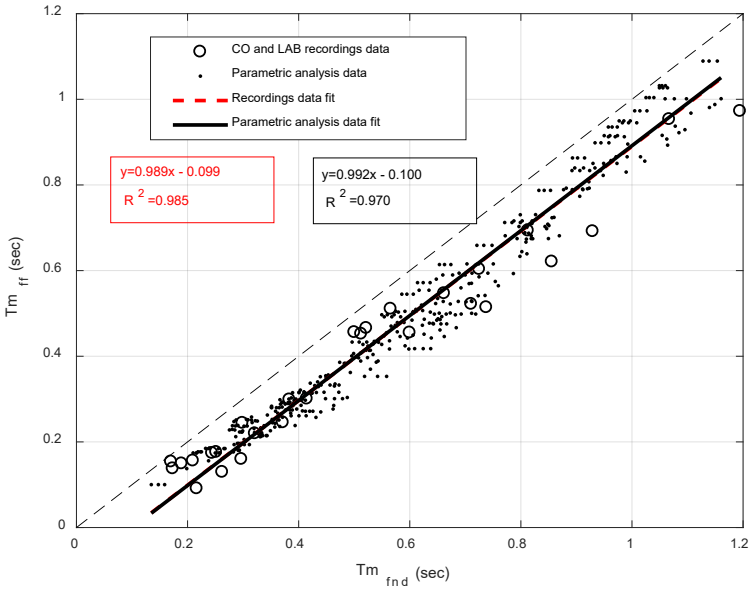

Fig. 14 Relationship between the mean period (T_m) of free-field and foundation motion

A final observation illustrated in Fig. 18 is the relationship between the frequency content of the free-field and the foundation motion, as described by their mean period (T_m) defined in equation 10. A linear relationship between T_{mff} and T_{mfnd} is suggested by both the recorded and analysis data. More specifically, both types of data reflect the filtering of high frequency components by the foundation by pointing to a higher value of T_{mfnd} with respect to T_{mff}. and a clear mean period shifting. The difference between the two mean periods is almost constant and equal to about 0.1 seconds for the data sets considered. This implies that the frequency content of high frequency motions arriving at a site will be modified significantly under the presence of the foundation. The similarity between the analysis and the recorded data in Fig. 18 denotes that the substructure analysis method implemented can capture, with a reasonable degree of accuracy, the modification of the frequency content of a free-field ground motion by the foundation.

6. CONCLUSIONS

The SSI effects on the foundation motion were studied for two sites in Greece presenting similar structural and soil characteristics as per the upper 30m and the respective values of V_{S30}. The investigation initially involved estimation of SSI effects directly from strong motion recordings from the two sites, where instrumentation existed at both the free-field and the lowest level of the buildings. Established methodologies were implemented (Kim and Stewart, 2003; Mikami et al., 2008) to estimate the transfer function between the foundation and the free-field motion. Moreover, the relationship between the two motions was investigated in terms of three different intensity measures (PGA, a_{rms}, I_A) and frequency content parameters expressed by means of the mean period T_m. The recorded data were supplemented by parametric substructure analysis results and a comparison between them was presented. The following conclusion were drawn:

- Strong motion recordings, from instrumented sites where ground motions are obtained both at the free-field and inside a nearby building, consist a valuable source of information for investigating the effect of soil-foundation-structure interaction on the recorded motions.
- The transfer functions that were based on the available records for the two sites (CO and LAB), clearly show the filtering of the high frequencies due to the presence of the foundation compared to the free-field motions. For the sites studied herein, classified as type C according to EC8, significant filtering was observed for frequencies higher than 4-5 Hz.
- Plotting intensity measures for both free-field and foundation motions reveals a linear relationship between them, for the range of intensities considered. The intensity of the free-field motion is found higher than that of the corresponding foundation motion, by an amount which depends on the intensity measure considered (49% for PGA, 70% for a_{rms} and 73% for I_A).

- The mean period of the free-field motion is increased when transferred to the foundation base by about of 0.1 seconds. This is a quantitative indication of the modification of the frequency content of free-field ground motions as a result of SSI.
- The sub-structure analysis method adopted for decoupling the kinematic and inertial SSI, even though quite simplified, captures some basic aspects of the recordings data observations. It matches reasonably well, on average, the recordings-based transfer function, the a_{rms} relationship between foundation and free-field motion, as well as, the frequency content alteration between the two. However, it overestimates the SSI effects when the *PGA* and I_A are employed as the IM of interest. Larger discrepancies for these cases are also observed for low mean period motions.
- The above conclusions are limited to the sites and events studied herein. Collection of a larger sample of recorded data from well documented stations, as well as, application of more sophisticated analysis methods, are of primary importance so that more refined predictions can be made. The results of this study, however, add further evidence about the influence of SSI on the records obtained at the base of instrumented buildings and pave the way for further discussion regarding the potential correction of such records when used in the framework of Ground Motion Prediction Equations and/or Seismic Hazard assessment.

Acknowledgements

The first author was financially supported by the General Secretariat for Research and Technology (GSRT) and the Hellenic Foundation for Research and Innovation (HFRI). This support is highly appreciated.

This research work was partially supported by the Scientific project (HELPOS MIS 5002697).

References

Arias, A. (1970), “A measure of earthquake intensity," in Seismic Design for Nuclear Power Plants (ed. R.J. Hansen), MIT Press, Cambridge, Massachusetts, pp. 438-483.

Bielak, J. (1974). “Dynamic behaviour of structures with embedded foundations”,Earthquake Engineering and Structural Dynamics, vol. 3, pp. 259-274.

Boore, D., M.,, Stewart, P., J.,, Seyhan, E. and Atkinson, G., M. (*2014*) NGA-West2 Equations for Predicting PGA, PGV, and 5% Damped PSA for Shallow Crustal Earthquakes. Earthquake Spectra: August 2014, Vol. 30, No. 3, pp. 1057-1085.

Conti, R., Morigi, M., Viggiani, G., (2017). “Filtering effect induced by rigid massless embedded foundations”, Bulletin of Earthquake Engineering, 15:1019 – 1035.

Conti, R., Morigi, M., Rovithis, E., Theodoulidis, N., Karakostas, C. (2018). “Filtering action of embedded massive foundations: New analytical expressions and evidence from 2 instrumented buildings”, Earthquake Engineering and Structural Dynamics 2018, vol. 47 pp. 1229–1249.

Darendeli, M. B. (2001). “Development of a new family of normalized modulus reduction and material damping curves”, Austin, Texas: The University of Texas.

Dobry, R. and Gazetas, G., (1986). “Dynamic response of arbitrary shaped foundations: experimental verification”,Journal of Geotechnical Engineering, ACSE, vol. 112(2), pp. 136-154.

Elsabee, F., Morray, J.P., Roesset, J.M. (1977). “Dynamic behavior of embedded foundations” Research Report R77-33, Massachusets Institute of Technology, Cambridge, Massachusetts.

CEN.European standard EN1998-1 (2005) Eurocode 8: Design of structures for earthquake resistance—part 1: general rules, seismic actions and rules for buildings. European Committee for Standardization, Brussels.

Engineering Geological Map of Greece (1993), Institute of Geology and Mineral Exploration (IGME), Athens, Greece.

Gazetas, G. (1991). “Formulas and charts for impedances of surface and embedded foundations”, Journal of Geotechnical Engineering, ASCE, 113(5), 458-475.

Gazetas, G., Koukis, G., Tselentis, A. (2004). “The earthquake of Lefkas 14.8.2003 – Collection/ Analysis of seismology, geological, geotechnical and structural data. – Failure analysis of Lefkada, Ligia, Nidri and Vasiliki ports (in Greek)”, National Technical University of Athens, Univeristy of Patras, EPPO research report.

599 Hossein, J., Pouran, F. F., (2017). “The effect of foundation embedment on net horizontal foundation input motion:
600 The case of strip foundation with incomplete contact to nearby medium”, Soil Dynamics & Earthquake
601 Engineering, vol. 96, pp. 35-48.
602 Idriss, I. M. (1990). “Response of soft soil sites during earthquakes”, Proceedings of H. Bolton Seed Memorial
603 Symposium, BiTech Publishers, Vancouver, British Columbia, Vol. 2, pp. 273-289.
604 Karakostas, C., Kontogiannis, G., Morfidis, K., Rovithis, E., Manolis, G., Theodoulidis, N., (2017). “Effect of soil-
605 structure interaction on the seismic response of an instrumented building during the Cephalonia, Greece earthquake
606 of 26-1-2014”, COMPDYN 2017, Rhodes Island, Greece, 15-17 June 2017.
607 Kausel, E., Whitman, R.V., Morray, J.P., Elsabee, F., (1978). “The spring method for embedded foundations”, Nuclear
608 Engineering and Design, vol. 48, pp. 377–392.
609 Kim, S. and Stewart, J.P., (2003). “Kinematic Soil-Structure Interaction from Strong Motion Recordings”, Journal of
610 Geotechnical and Geoenvironmental Engineering, vol. 129, pp. 323-335.
611 Kottke, A. R., Wang, X., Rathje, E. M., (2013). “Technical manual for Strata”, Geotechnical Engineering Center,
612 Department of Civil, Architectural and Environmental Engineering, University of Texas.
613 Kramer, S.L., (1996). “Geotechnical Earthquake Engineering”, Prentice-Hall, U.S.A., ISBN: 0133749436.
614 Lesgidis, N., Kwon, O.-S., Sextos, A.G. (2015). “A time-domain seismic SSI analysis method for inelastic bridge
615 structures through the use of a frequency-dependent lumped parameter model”, *Earthquake Engineering and*
616 *Structural Dynamics*, vol. 44(13), pp. 2137-2156.
617 Lesgidis, N., Sextos, A.G., Kwon, O.-S. (2016). “Influence of frequency-dependent soil–structure interaction on the
618 fragility of R/C bridges”, *Earthquake Engineering and Structural Dynamics*, vol. 46 (1), pp. 139-158.
619 Lesgidis, N., Sextos, A.G. and Kwon, O.-S. (2018). “A frequency- and intensity-dependent macroelement for reduced
620 order soil-structure interaction analysis”, *Earthquake Engineering and Structural Dynamics,* vol. 47(11), pp. 2172-
621 2194.
622 Luco, J. E., (1974). “Impedance functions for rigid foundations on a layered medium”, Nuclear Engineering and
623 Design, vol. 31(2), pp. 204-217.
624 Luco, J. E. and Wong, H. L. (1987). “Seismic response of foundations embedded in a layered half-space” Earthquake
625 Engineering and Structural Dynamics, vol. 15, pp. 233-247.
626 Luco, J. E., Anderson, J. G. and Georgevich, M. (1990). “Soil-structure interaction effects on strong motion
627 accelerograms recorded on instrument shelters”, Earthquake Engineering and Structural Dynamics, vol. 19, pp.
628 119–131.
629 Manakou, M., Apostolidis, P., Raptakis, D., Pitilakis, K., (2008). “Determination of soil structure in the broader urban
630 Thessaloniki area”, 3rd Hellenic Conference of Earthquake Engineeringand Engineering Seismology, Athens,
631 Greece, paper No 1978 (in Greek).
632 Mikami, A., Stewart, J.P., Kamiyama, M., (2008). “Effect of time series analysis protocols on transfer functions
633 calculated from earthquake accelerograms”, Soil Dynamics and Earthquake Engineering, vol. 28, pp. 695–706.
634 Mylonakis, G., Nikolaou, S., Gazetas, G., (2006). “Footings under seismic loading: Analysis anddesign issues with
635 emphasis on bridge foundations”, Soil Dynamics and Earthquake Engineering, vol. **26**(9), pp. 824-853.
636 Nakamura, Y., (1989). A method for Dynamic Characteristics Estimation of Subsurface using Microtremor on the
637 Ground Surface. QR Railway Tech. Res. Inst. 30, no. 1, 25-33.
638 Pais, A., Kausel, E., (1988). “Approximate formulas for dynamic stiffnesses of rigid foundations”, Soil Dynamics and
639 Earthquake Engineering, vol 7(4), pp. 213-227.
640 Pandit., S. M. (1991) “Modal and spectrum analysis”, Wiley, New York, ISBN:9780899307015.
641 Rathje, E. M., Abrahamson, N. A., Bray, J. D., (1998). “Simplified frequency content estimates of earthquake ground
642 motions”, Journal of Geotechnical and Geoenvironmental Engineering, ASCE, vol. 124(2), pp.150–159.
643 Sarma, S. K. and Srbulov, M. (1996). “A simplified method for prediction of kinematic soil–foundation interaction
644 effects on peak horizontal acceleration of arigid foundation”, Earthquake Engineering and Structural Dynamics,
645 vol. 25, pp. 815-836.
646 Somerville, P. G., McLaren, J. P., Sen, M. K., and Helmberger, D. V. (1991). “The influence of site conditions on the
647 spatial incoherence of ground motions.” Structural Safety, 10(1-3), 1-13.
648 Stewart, J. P., Kim, S., Bielak, J., Dobry, R., and Power, M. (2003). “Revisions to soil structure interaction procedures
649 in NEHRP design provisions”, Earthquake Spectra, vol. 19(3), pp. 677-696.
650 Stewart, J. P., Seed, R. B., Fenves, G. L. (1998). “Empirical evaluation of inertial soil-structure interaction effects”,
651 PEERC, Report No. PEER – 98/07.
652 Talaganov, K. and Cubrinovski, M. (1991). "Soil-structure interaction effects based on recorded strong motions during
653 earthquakes", International Conferences on Recent Advances in Geotechnical Earthquake Engineering and Soil
654 Dynamics*,* paper 42.

655 Toro, G. R. (1995). “Probabilistic models of site velocity profiles for generic and site-specific ground-motion
656 amplification studies”, Upton, New York: Brookhaven National Laboratory.
657 Trifunac, M. D., (1972). “Interaction of a shear wall with the soil for incident plane SH waves”, Bulletin of the
658 Seismological Society of America, vol. 62, No.1, pp. 63–83.
659 Veletsos, A. S. and Meek, J. W. (1974). “Dynamic behaviour of building-foundation systems”,Earthquake
660 Engineering and Structural Dynamics, vol. 3, pp. 121-138.
661 Veletsos. A.S., Prasad, A.M., W.H. Wu, (1997). “Transfer functions for rigid rectangular foundations”, Earthquake
662 Engineering and Structural Dynamics, vol.26, pp. 5-17.
663 Wolf, J. P. and Somaini, D. R. (1986). “Approximate dynamic model of embedded foundation in time domain”,
664 Earthquake Engineering and Structural Dynamics, vol. 14, pp. 683-703.
665 Yamada, M., Miyoshi, M., Horike, M., (2016). “Evaluation of effective input motions to structures using seismograms
666 recorded at structure foundations and free field”, 5th IASPEI/IAEE International Symposium, August 15 -17.
667